Structure of *Geobacter* pili reveals secretory rather than nanowire behaviour

https://doi.org/10.1038/s41586-021-03857-w

Received: 28 February 2020

Accepted: 28 July 2021

Published online: 01 September 2021

Check for updates

Yangqi Gu[1,2,5], Vishok Srikanth[1,3,5], Aldo I. Salazar-Morales[1,3], Ruchi Jain[1,3], J. Patrick O'Brien[1,3], Sophia M. Yi[1,3], Rajesh Kumar Soni[4], Fadel A. Samatey[1,3], Sibel Ebru Yalcin[1,3] & Nikhil S. Malvankar[1,3]✉

Extracellular electron transfer by *Geobacter* species through surface appendages known as microbial nanowires[1] is important in a range of globally important environmental phenomena[2], as well as for applications in bio-remediation, bioenergy, biofuels and bioelectronics. Since 2005, these nanowires have been thought to be type 4 pili composed solely of the PilA-N protein[1]. However, previous structural analyses have demonstrated that, during extracellular electron transfer, cells do not produce pili but rather nanowires made up of the cytochromes OmcS[2,3] and OmcZ[4]. Here we show that *Geobacter sulfurreducens* binds PilA-N to PilA-C to assemble heterodimeric pili, which remain periplasmic under nanowire-producing conditions that require extracellular electron transfer[5]. Cryo-electron microscopy revealed that C-terminal residues of PilA-N stabilize its copolymerization with PilA-C (to form PilA-N–C) through electrostatic and hydrophobic interactions that position PilA-C along the outer surface of the filament. PilA-N–C filaments lack π-stacking of aromatic side chains and show a conductivity that is 20,000-fold lower than that of OmcZ nanowires. In contrast with surface-displayed type 4 pili, PilA-N–C filaments show structure, function and localization akin to those of type 2 secretion pseudopili[6]. The secretion of OmcS and OmcZ nanowires is lost when *pilA-N* is deleted and restored when PilA-N–C filaments are reconstituted. The substitution of *pilA-N* with the type 4 pili of other microorganisms also causes a loss of secretion of OmcZ nanowires. As all major phyla of prokaryotes use systems similar to type 4 pili, this nanowire translocation machinery may have a widespread effect in identifying the evolution and prevalence of diverse electron-transferring microorganisms and in determining nanowire assembly architecture for designing synthetic protein nanowires.

The hypothesis that PilA-N filaments function as nanowires[1] is open to question[7] because: (1) the deletion of *pilA-N* also inhibits the extracellular translocation of OmcS[8,9] and OmcZ[9], which form nanowires that are essential for extracellular electron transfer to iron oxide and electrodes, respectively[7]; (2) the presence of PilA-N in a filament of wild-type cells has not been established (instead, it has only been inferred from indirect evidence, such as the presence of PilA-N monomer in filament preparations that also contain OmcS nanowires[2]); (3) conduction along the length of a purified PilA-N filament has not been demonstrated; and (4) theoretical studies did not find substantial conductivity in a hypothetical PilA-N filament structure, except when aromatic residues were assumed to be within 3–4 Å of each other (ref. [7] and references therein).

Splitting *pilA* into *pilA-N* and *pilA-C*

The *G. sulfurreducens* genome contains two neighbouring genes that are related to *pilA*[9] (Fig. 1a). The first gene is annotated as *pilA-N* (GSU1496) because it encodes a 61-amino-acid protein that shows high amino acid sequence identity to the N-terminal α-helix of previously reported type 4 pilin proteins, but lacks the C-terminal globular domain that is found in type 4 pili (T4P)[9] (Supplementary Fig. 1). Immediately downstream of *pilA-N* is a gene annotated as *pilA-C* (GSU1497) because it was previously thought to be the C-terminal globular domain that is missing from PilA-N[9] (Fig. 1a). PilA-N was previously hypothesized to be the only protein within *G. sulfurreducens* pili[1], owing to the lack of sequence similarity among PilA-C and the globular domain of type 4 pilin proteins (even though all globular domains of T4P show low sequence conservation (Supplementary Fig. 1), but high structural conservation, extending to the predicted structure of PilA-C[10]). Gene fission of type 4 pilins is widespread in *Desulfuromonadales* species, including in the *Geobacteraceae* and other iron-reducing bacteria[10]. Our phylogenetic analysis of a fused PilA-N and PilA-C sequence showed an independent line of descent along with PilA-N–C subunits of other *Geobacter* species, which indicates that *Geobacter* PilA-N–C are evolutionarily distant from

[1]Microbial Sciences Institute Yale University, West Haven, CT, USA. [2]Department of Molecular, Cellular and Developmental Biology, Yale University, New Haven, CT, USA. [3]Department of Molecular Biophysics and Biochemistry, Yale University, New Haven, CT, USA. [4]Proteomics and Macromolecular Crystallography Shared Resource, Herbert Irving Comprehensive Cancer Center, Columbia University Irving Medical Center, New York, NY, USA. [5]These authors contributed equally: Yangqi Gu, Vishok Srikanth. ✉e-mail: nikhil.malvankar@yale.edu

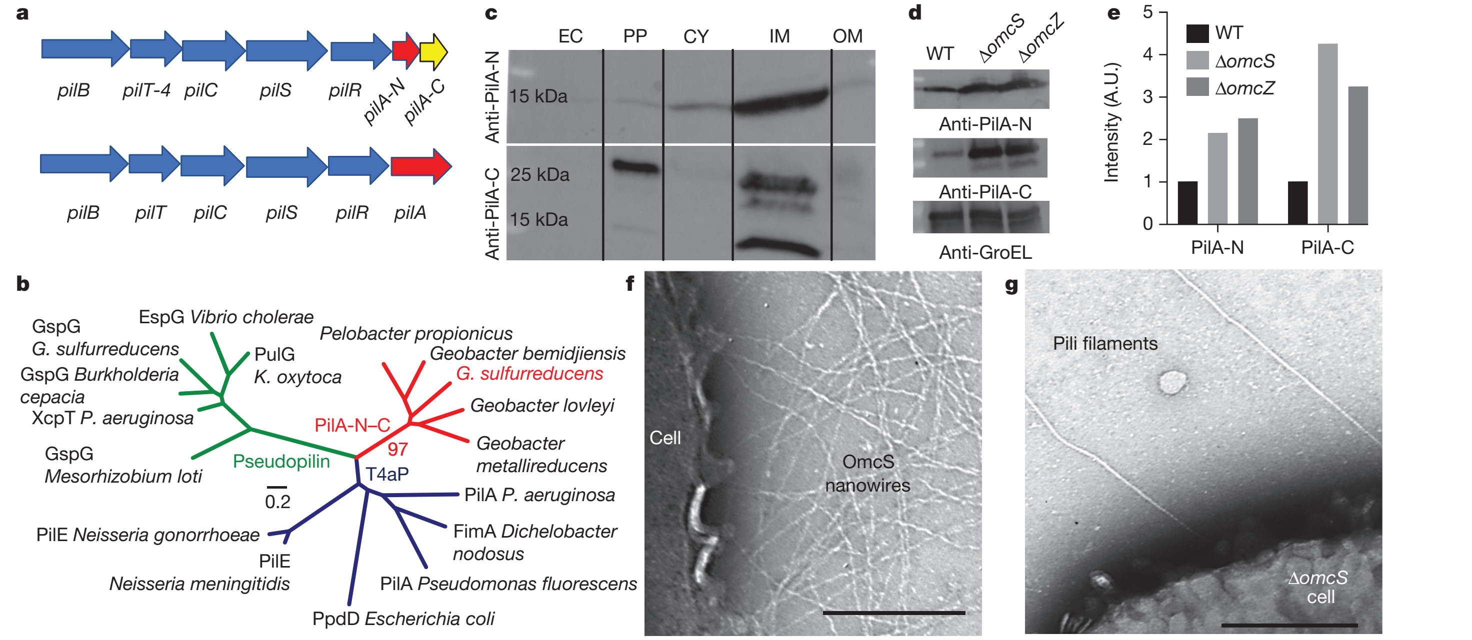

Fig. 1 | Discovery and identification of *G. sulfurreducens* pili. a, Genomic organization of type 4 pili (T4P) biosynthesis genes in *G. sulfurreducens* (top) and *Myxococcus xanthus* (bottom). **b**, Phylogenetic distance tree derived from amino acid sequence alignments, 1 showing the relationship of *Geobacter* PilA-N-C pili and type 4a pilins (T4aP, blue branches) and pseudopilins (green branches) of other bacteria. See Supplementary Fig. 1 for details. **c**, Immunoblot of subcellular fractionation for PilA-N (about 6.5 kDa) and PilA-C (about 11 kDa) in wild-type cells. EC, extracellular; PP, periplasm; CY, cytoplasm; IM, inner membrane, OM, outer membrane. For gel source data, see Supplementary Fig. 4. **d**, **e**, Immunoblot for PilA-N and PilA-C in cell lysates (**d**) with quantification (**e**). Control, the cytoplasmic protein GroEL. For gel source data, see Supplementary Fig. 15. WT, wild type. **f**, Negative-stain TEM image of wild-type *G. sulfurreducens* cell showed only OmcS filaments on the cell surface. **g**, Pili-like filaments emanated from *ΔomcS* cell. Scale bars, 100 nm (**f**), 200 nm (**g**).

both T4P and pseudopili of type 2 secretion systems (T2SS) (Fig. 1b, Supplementary Fig. 1).

Discovery and identification of pili

We grew *G. sulfurreducens* wild-type cells using anodes of microbial fuel cells as the sole electron acceptors[11]. These conditions require extracellular electron transport over hundreds of cell lengths, and therefore represent an ideal nanowire-producing condition[5,7]. Purified filament preparations from wild-type cells grown under these nanowire-producing conditions did not show either PilA-N or PilA-C using immunoblotting (Supplementary Table 1), in agreement with previous cryo-electron microscopy (cryo-EM) analyses that did not find any T4P-like filaments[2,4]. We further analysed subcellular fractions of wild-type cells with anti-PilA-N antibodies, and found that PilA-N is associated mainly with the inner membrane and is absent from the extracellular fractions. PilA-C is also membrane-associated and absent from the extracellular fractions of wild-type cells[12] (Fig. 1c). Control experiments using antibodies against the cytoplasmic protein GroEL confirmed that there is little or no cross-contamination in these subcellular fractions, as only cytoplasmic fractions showed GroEL (Supplementary Fig. 2). These studies suggested that in wild-type *G. sulfurreducens*, PilA-N and PilA-C remain periplasmic and are anchored to the inner membrane, akin to T2SS pseudopili that form a membrane-associated filament structure to secrete proteins through elongation–retraction cycles[6]. Similar to the overexpression of pseudopilins causing the pseudopilus filaments to extend beyond the outer membrane[6,13,14], we hypothesized that *G. sulfurreducens* filaments may extend outside the cell surface if PilA-N and PilA-C proteins were present at levels higher than those observed in the wild type. Both *ΔomcS* and *ΔomcZ* cells, which lack nanowire-forming cytochromes, showed an increased abundance of PilA-N and PilA-C, and we found pili-like filaments on the surfaces of these cells by negative-stain transmission electron microscopy (TEM) (Fig. 1d–g, Extended Data Fig. 1a–c). Overexpressing PilA-N and PilA-C from a plasmid in wild-type *G. sulfurreducens* also yielded extracellular pilus-like filaments (Extended Data Fig. 2) with a smooth morphology that is distinct from the sinusoidal morphology of cytochrome nanowires[2,4] (Figs. 1f, g, 2a, b). In contrast to cytochrome nanowires[2,4] or T4P[15], which need to be removed from cells through vortexing or blending, these pili-like filaments were loosely attached to cells (akin to pseudopili[14]) and were shed in the medium. Therefore, cell-free supernatant of *ΔomcS* cells was concentrated to purify PilA-N–C filaments (Extended Data Fig. 1c–f).

PilA-N and PilA-C form a heterodimeric pilin

Analysis of cryo-EM images of these pilus-like filaments using the iterative helical real-space reconstruction approach yielded a map at about 3.8 Å resolution according to the 'gold standard' map:map and 3.9 Å according to the model:map Fourier shell correlation (Supplementary Fig. 3). The overall structural features of the filament are similar to T4P, with a helical core and globular head domain that are arranged within a right-handed helix with helical rise of about 10.4 Å and rotation of 89.1° (Fig. 2c). The PilA-N sequence could be threaded through the helical core of the map and the PilA-C sequence could be threaded through the globular domains on the outer surface (Fig. 2d, Extended Data Fig. 3). Overall, the excellent agreement between the model and the map, the good fit of side chains and the refinement statistics (Supplementary Table 2) confirm that PilA-N and PilA-C form a heterodimer that polymerizes into a filament (Fig. 2e, Supplementary Videos 1–3).

PilA-N is composed of two α-helices: segments F1–L16 form an N-terminal helix and S25–F51 form a C-terminal helix, and are linked by a short coil (Fig. 2d). A staggered helical array of PilA-N subunits forms the core of the PilA-N–C filament (Fig. 2e). PilA-C consists of

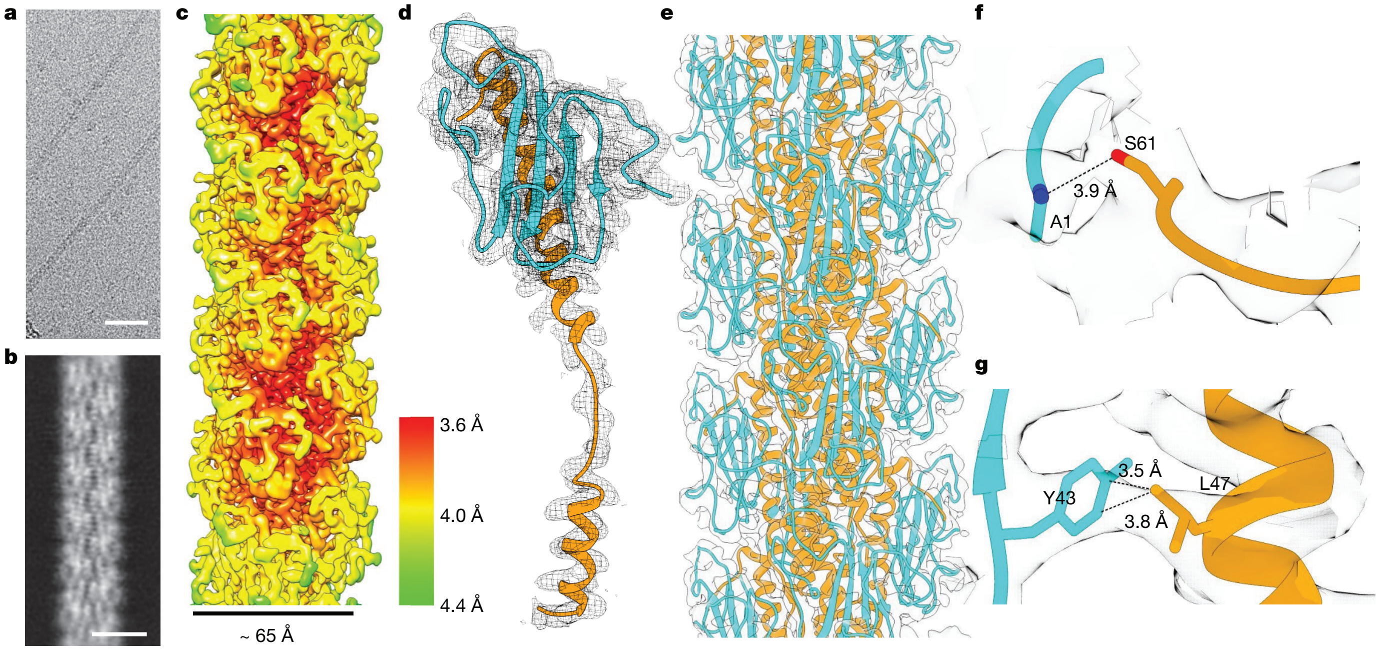

Fig. 2 | PilA-N recruits PilA-C to form a heterodimer that polymerizes into a filament. a–c, Cryo-EM micrograph (**a**), two-dimensional average (**b**) and resolution distribution of a density map (**c**) of a PilA-N–C filament. Scale bars, 30 nm (**a**), 5 nm (**b**). **d**, **e**, PilA-N (orange) and PilA-C (cyan) form a heterodimer (**d**) that polymerizes into a filament (**e**). **f**, Charge interactions between S61 of PilA-N and A1 of PilA-C. **g**, Hydrophobic interactions between PilA-N and PilA-C.

four anti-parallel β-strands surrounded by a web of loops (Fig. 2d). It binds at the second α-helix of PilA-N through an extensive network of electrostatic and hydrophobic interactions that stabilizes the PilA-N–C heterodimer. In addition to extensive contacts between PilA-C and the C-terminal helix of PilA-N, the C-terminal 5 residues of PilA-N protrude and are held between two 'flaps' of PilA-C (Extended Data Fig. 4). The N terminus of PilA-C (Ala1) interacts with the C terminus of PilA-N (Ser61) through hydrogen bonding or possibly a salt bridge (Fig. 2f). Our structure explains the yeast two-hybrid assay with PilA-N and PilA-C monomers[12], which found that reversing the charged sites in PilA-N at D39, R41 and K44 and E60 inhibits its interaction with PilA-C by disrupting electrostatic interactions or introducing clashes between the monomers, whereas reversing the charges at K30, E48, D53 and D54does not (Extended Data Fig. 5d).

In addition to electrostatic interactions, hydrophobic interactions—such as the interactions between L47 from PilA-N and Y43 from PilA-C (Fig. 2g)—also appeared critical for filament stability. The filament is organized mainly through interactions between adjacent PilA-N subunits (Extended Data Fig. 5a, c), with little direct interaction between copies of PilA-C within the filament (Fig. 2e). The PilA-N–C filament did not show the post-translational modifications that have previously been reported for the PilA-N monomer[16]. Rather, we observed N-terminal methylation of PilA-N (Extended Data Fig. 6b), as seen in other T4P[15], and extra density around S94 for PilA-C. A glycoprotein western assay suggested that this density could be attributed to O-linked glycosylation (Extended Data Fig. 6c, d). Such glycosylation on a serine residue near the C terminus is commonly observed in other T4P[17,18], in which it is important in pilus biogenesis[19]. As the N terminus of PilA-N is primarily composed of hydrophobic residues, binding to PilA-C prevents the exposure of the hydrophobic side chains to the aqueous environment (Fig. 2e, Extended Data Fig. 5b).

PilA-N–C filaments are pseudopili-like

Geobacter sulfurreducens PilA-N–C filaments lack several hallmarks of T4P structure[20] and instead show similarity to the structure of T2SS pseudopili[21] (Extended Data Fig. 7a, b). First, a salt bridge between N-terminal F1 and E5 of neighbouring subunits is highly conserved among all T4P and is crucial for their stability and assembly[20] (Extended Data Fig. 7b). However, this salt bridge is absent in *G. sulfurreducens* PilA-N–C filaments. Instead, the N-terminal amine at F1 interacts with E5 from the same subunit to neutralize the buried charge. Adjacent PilA-N subunits are primarily stabilized by hydrophobic interactions (Extended Data Fig. 7b), as has previously been observed in the pseudopili from *Klebsiella oxytoca*[21]. Second, the α–β loop in the globular head domain, which is involved in the subunit–subunit interactions in assembled T4P filaments[20], is absent in the PilA-N–C filament. Third, the D-region in the globular head domain contains a disulfide bridge that is essential for assembly of some T4P filaments[20], but is notably absent in pseudopili[21] and in PilA-N–C (Extended Data Fig. 7a). The lack of disulfide bridges—combined with the observation that PilA-N–C filaments are easily detached under conditions in which they extend from the cell—suggested that the biological function of PilA-N–C filaments is not as a durable, extracellular structure similar to T4P, but rather as a comparatively fragile, periplasmic assembly akin to T2SS pseudopili[21]. Purified PilA-N–C filaments further exhibit melting of secondary structure features, denaturation and disassembly at much lower temperatures than T4P[22] (Extended Data Fig. 8). PilA-N–C filaments are very loosely attached to cells and readily dissociated into pilin subunits under the buffer conditions that are widely used to purify T4P[20], or upon the addition of mild detergents such as deoxycholate. All these studies demonstrate a substantially lower stability of PilA-N–C compared to T4P filaments.

Probably owing to this reduced stability, *G. sulfurreducens* PilA-N–C pili do not show any behaviours that are consistent with typical T4P functions (such as adhesion and twitching motility) (Extended Data Fig. 7c, d), even under the artificial conditions that result in their display on the cell surface. Wild-type, *ΔomcS* and *ΔomcZ* mutant strains showed a very low attachment to glass, comparable to *ΔpilA-N* cells (Extended Data Fig. 7c). Replacing the chromosomal *G. sulfurreducens pilA-N* with T4P-forming *Pseudomonas aeruginosa pilA* ([23], hereafter, *Gs-Pa*) increased the attachment by 100-fold (Extended Data Fig. 7c). *Geobacter sulfurreducens* strains displayed negligible twitching motility compared to *P. aeruginosa* (Extended Data Fig. 7d) and were comparable to *P. aeruginosa ΔpilA*. These data are therefore more consistent with

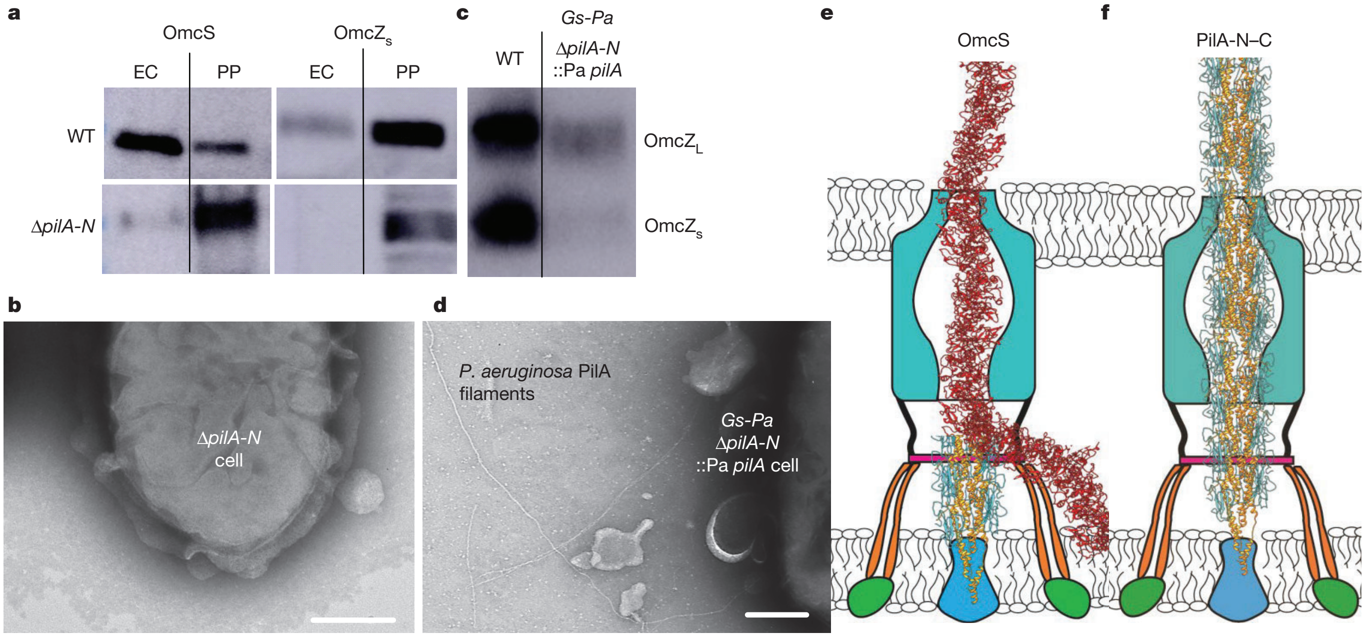

Fig. 3 | *Geobacter sulfurreducens* PilA-N–C pili are involved in the translocation of OmcS and OmcZ nanowires. a, Immunoblot for subcellular fractionation of OmcS (about 45 kDa) and $OmcZ_s$ (about 30 kDa) in wild-type cells. EC, extracellular; PP, periplasmic, showing the lack of secretion of OmcS and $OmcZ_s$ in the *ΔpilA-N* strain. For gel source data, see Supplementary Fig. 9. **b**, Negative-stain TEM images showed that the *ΔpilA-N* strain lacked OmcS filaments. Scale bar, 200 nm. **c**, Lack of nanowire-forming $OmcZ_s$ in filament preparations of a strain in which *pilA-N* was replaced with *pilA* of *P. aeruginosa* (*Gs-Pa* cells). Cells still produce intracellular $OmcZ_L$ (about 50 Da). For gel source data, see Supplementary Fig. 10. *Gs*, *Geobacter sulfurreducens*; *Pa*, *P. aeruginosa*. **d**, TEM image of *ΔpilA-N* cell expressing *P. aeruginosa pilA*. Scale bar, 200 nm. **e**, **f**, Model for PilA-N–C-assisted secretion of nanowires in wild-type cells (**e**) and extracellular extension of PilA-N–C pili in the absence of nanowires in *ΔomcS ΔomcZ* cells (**f**).

wild-type *G. sulfurreducens* expressing periplasmic pseudopili rather than surface-displayed T4P filaments.

PilA-N–C has low electronic conductivity

Biologically relevant electron transport along extracellular PilA-N-only filaments has long been postulated as a unique function of *Geobacter* T4P, separate from other classical T4P functions[1]. However, computational studies have predicted very low conductivity in a theoretical PilA-N-only filament model using either the nuclear magnetic resonance monomer structure or a hypothetical homology-based model that has not been observed in nature (ref. [7] and references therein). Furthermore, there is no direct experimental evidence to support the existence of PilA-N filaments consistent with these hypothetical structures in wild-type *Geobacter*. It has previously been proposed that the thin filaments observed in some cryo-EM images are PilA-N filaments[3] (Extended Data Fig. 9a). However, our analysis of such images revealed that the morphologically similar filaments we observed are DNA and not pili (Extended Data Fig. 9b–e).

Some theoretical models of PilA-N had suggested that aromatic side chains could be 3–4 Å from each other to form π-stacking interactions[24] (Extended Data Fig. 7e). A computational study performed on the basis of these theoretical models of π-stacked PilA-N has a predicted conductivity of 65–330 mS cm^{-1} (ref. [7] and references therein). However, conductivity measurements and theoretical studies yielded very low conductivity (about 1 μS cm^{-1}) in synthetic proteins that contain such π-stacking of aromatic side chains[25]. Furthermore, the cryo-EM structure of the PilA-N–C filament showed that approximately 10 Å gaps exist between aromatic residues along the PilA-N core of the filament (Extended Data Fig. 7f). Because the electron transfer rate decreases with increasing distance, the PilA-N–C structure thus suggested very low conductivity for these pili, as predicted by theoretical studies of a similar PilA-N structure based on other T4P structures[7].

To further evaluate whether *G. sulfurreducens* pili can function as nanowires, we compared the direct current conductivity of individual PilA-N–C filaments with OmcS nanowires. We used atomic force microscopy to locate individual pili that bridged two gold electrodes (Extended Data Fig. 7g). Atomic force microscopy showed smooth-surfaced structures with 6-nm heights, consistent with the filaments characterized by cryo-EM. Our purified pilus samples did not contain other filament-forming proteins such as OmcS and OmcZ, as confirmed by mass spectrometry (Extended Data Fig. 1d–f). Our conductivity measurements of individual filaments fully hydrated in buffer yielded low current values[2] for PilA-N–C filaments, comparable to buffer alone (Extended Data Fig. 7h). The observed conductivity was about 1 mS cm^{-1}—20-fold lower than OmcS nanowires[2] measured under conditions identical to pilus measurements (Extended Data Fig. 7i). As OmcZ nanowires are 1,000-fold more conductive than OmcS nanowires[4], our measurements show that *G. sulfurreducens* pili are 20,000-fold less conductive than OmcZ nanowires. Previous physiological studies have shown that *ΔomcS* cells cannot transfer electrons to extracellular iron and electrodes, and *ΔomcZ* cells cannot transfer electrons to electrodes beyond a few monolayers of cells[7]. The *ΔomcS* cells can adapt after prolonged growth on electrodes, but *ΔomcZ* cells cannot[5,7]. As both *ΔomcS* and *ΔomcZ* cells were found to show PilA-N–C filaments on their surfaces (Fig. 1g and Extended Data Fig. 1), these studies suggest that PilA-N–C filaments are unlikely to function as nanowires and that the above-mentioned phenotypes can be explained using OmcS and OmcZ nanowires[7]. It remains possible that synthetic *pilA-N* assembles into a filament under artificial conditions (ref. [7] and references therein). However, the conductivity of individual synthetic filaments has not been demonstrated along their length, only across their diameter[7]. Furthermore, such PilA-N-only filaments are unlikely to be responsible for biologically relevant electron transfer, considering that we did not find any filament containing PilA-N located extracellularly under nanowire-producing conditions (Supplementary Table 1).

Nanowire secretion requires PilA-N–C pili

The lack of either nanowire or typical T4P functions suggests that the biological role of PilA-N–C filaments is not compatible with previous descriptions of *Geobacter* T4P function. In addition to classical T2SS, *G. sulfurreducens* also contain incomplete T2SS, lacking typical components of the machinery[6]. Deletion of the T2SS pseudopilin gene for the incomplete T2SS was previously found not to affect the translocation of outer-surface cytochromes[26]. Furthermore, other species that use classical T2SS for extracellular translocation of *c*-type cytochromes[27] do not show any secretion defect in the absence of pili[28]. In *G. sulfurreducens*, deletion of *pilA-N* does inhibit the extracellular translocation of OmcS and OmcZ[8,9], which underscores the involvement of pili in the secretion of nanowire-forming cytochromes. Our subcellular localization experiments revealed that both OmcS and OmcZ are present in the extracellular fraction of wild-type cells but remain in the periplasm for *ΔpilA-N* cells (Fig. 3a). These results suggested a translocation defect for OmcS and OmcZ in *ΔpilA-N* cells. Consistent with these studies, TEM showed OmcS nanowires on the surface of wild-type cells (Fig. 1f) but not on the surface of *ΔpilA-N* cells (Fig. 3b). Notably, *in trans* expression of an episomal copy of wild-type *pilA-N* and *pilA-C* in *ΔpilA-N* cells (hereafter, Δ*pilA*-N/*pilA*-N-C) reassembled the PilA-N–C filaments on the bacterial surface and restored secretion for both OmcS and OmcZ nanowires (Extended Data Fig. 10). As the primarily periplasmic localization (Fig. 1c) and the filament structure (Extended Data Fig. 7a) of the PilA-N–C are similar to T2SS pseudopili, these cytochrome localization studies further suggest that PilA-N–C filaments could be functioning similar to pseudopili by translocating the OmcS and OmcZ nanowires from the periplasm to the outer cell surface.

To further evaluate the function of the PilA-N–C filament, we analysed the localization of cytochromes in the *Gs-Pa* strain[23] (Fig. 3c, d). This strain cannot transport electrons extracellularly to electrodes in microbial fuel cells[23]. Our TEM images showed T4P-like filaments in *Gs-Pa* cells (Fig. 3d). However, we found that filament preparations from electrode-grown *Gs-Pa* cells did not show the extracellular form of OmcZ ($OmcZ_s$) that assembles into nanowires[4] and only showed the periplasmic form of OmcZ ($OmcZ_L$), which confirms that the cells were able to produce OmcZ but could not secrete it (Fig. 3c). This lack of $OmcZ_s$ could explain why these strains cannot transfer electrons to electrodes as $OmcZ_s$ is essential for electricity production[4,7]. By contrast, OmcS was translocated extracellularly by *Gs-Pa* cells[23], similarly to a strain in which *pilA-N* and *pilA-C* genes were fused[29]. Our studies thus show that the unique PilA-N–C filaments are essential for the translocation of OmcZ nanowires and are capable of secreting cytochromes without being displayed on the cell surface in a manner analogous to T2SS pseudopili[6,13,14]. The translocation of OmcS can be rescued as long as a T4P is present, probably because of a similar secretory role for T4P[30].

Online content

Any methods, additional references, Nature Research reporting summaries, source data, extended data, supplementary information, acknowledgements, peer review information; details of author contributions and competing interests; and statements of data and code availability are available at https://doi.org/10.1038/s41586-021-03857-w.

1. Reguera, G. et al. Extracellular electron transfer via microbial nanowires. *Nature* **435**, 1098–1101 (2005).
2. Wang, F. et al. Structure of microbial nanowires reveals stacked hemes that transport electrons over micrometers. *Cell* **177**, 361–369 (2019).
3. Filman, D. J. et al. Cryo-EM reveals the structural basis of long-range electron transport in a cytochrome-based bacterial nanowire. *Commun. Biol.* **2**, 219 (2019).
4. Yalcin, S. E. et al. Electric field stimulates production of highly conductive microbial OmcZ nanowires. *Nat. Chem. Biol.* **16**, 1136–1142 (2020).
5. Malvankar, N. S. et al. Tunable metallic-like conductivity in microbial nanowire networks. *Nat. Nanotechnol.* **6**, 573–579 (2011).
6. Michel, G. P. & Voulhoux, R. in *Bacterial Secreted Proteins: Secretory Mechanisms and Role in Pathogenesis* (ed. Wooldridge, K.) 67–92 (Caister Academic, 2009).
7. Yalcin, S. E. & Malvankar, N. S. The blind men and the filament: understanding structures and functions of microbial nanowires. *Curr. Opin. Chem. Biol.* **59**, 193–201 (2020).
8. Liu, X., Zhuo, S., Rensing, C. & Zhou, S. Syntrophic growth with direct interspecies electron transfer between pili-free *Geobacter* species. *ISME J.* **12**, 2142–2151 (2018).
9. Richter, L. V., Sandler, S. J. & Weis, R. M. Two isoforms of *Geobacter sulfurreducens* PilA have distinct roles in pilus biogenesis, cytochrome localization, extracellular electron transfer, and biofilm formation. *J. Bacteriol.* **194**, 2551–2563 (2012).
10. Shu, C., Xiao, K., Yan, Q. & Sun, X. Comparative analysis of type IV pilin in *Desulfuromonadales*. *Front. Microbiol.* **7**, 2080 (2016).
11. O'Brien, J. P. & Malvankar, N. S. A simple and low-cost procedure for growing Geobacter sulfurreducens cell cultures and biofilms in bioelectrochemical systems. *Current Protoc. Microbiology* **43**, A.4K.1–A.4K.27 (2017).
12. Liu, X., Zhan, J., Jing, X., Zhou, S. & Lovley, D. R. A pilin chaperone required for the expression of electrically conductive *Geobacter sulfurreducens* pili. *Environ. Microbiol.* **21**, 2511–2522 (2019).
13. Vignon, G. et al. Type IV-like pili formed by the type II secreton: specificity, composition, bundling, polar localization, and surface presentation of peptides. *J. Bacteriol.* **185**, 3416–3428 (2003).
14. Durand, E. et al. XcpX controls biogenesis of the *Pseudomonas aeruginosa* XcpT-containing pseudopilus. *J. Biol. Chem.* **280**, 31378–31389 (2005).
15. Wang, F. et al. Cryoelectron microscopy reconstructions of the *Pseudomonas aeruginosa* and *Neisseria gonorrhoeae* type IV pili at sub-nanometer resolution. *Structure* **25**, 1423–1435 (2017).
16. Richter, L. V., Franks, A. E., Weis, R. M. & Sandler, S. J. Significance of a posttranslational modification of the PilA protein of *Geobacter sulfurreducens* for surface attachment, biofilm formation, and growth on insoluble extracellular electron acceptors. *J. Bacteriol.* **199**, e00716-16 (2017).
17. Parge, H. E. et al. Structure of the fibre-forming protein pilin at 2.6 Å resolution. *Nature* **378**, 32–38 (1995).
18. Harvey, H. et al. *Pseudomonas aeruginosa* defends against phages through type IV pilus glycosylation. *Nat. Microbiol.* **3**, 47–52 (2018).
19. Vik, Å. et al. Insights into type IV pilus biogenesis and dynamics from genetic analysis of a C-terminally tagged pilin: a role for O-linked glycosylation. *Mol. Microbiol.* **85**, 1166–1178 (2012).
20. Craig, L., Pique, M. E. & Tainer, J. A. Type IV pilus structure and bacterial pathogenicity. *Nat. Rev. Microbiol.* **2**, 363–378 (2004).
21. López-Castilla, A. et al. Structure of the calcium-dependent type 2 secretion pseudopilus. *Nat. Microbiol.* **2**, 1686–1695 (2017).
22. Li, J., Egelman, E. H. & Craig, L. Structure of the *Vibrio cholerae* type IVb Pilus and stability comparison with the *Neisseria gonorrhoeae* type IVa pilus. *J. Mol. Biol.* **418**, 47–64 (2012).
23. Liu, X. et al. A *Geobacter sulfurreducens* strain expressing *Pseudomonas aeruginosa* type IV pili localizes OmcS on pili but is deficient in Fe(III) oxide reduction and current production. *Appl. Environ. Microbiol.* **80**, 1219–1224 (2014).
24. Xiao, K. et al. Low energy atomic models suggesting a pilus structure that could account for electrical conductivity of *Geobacter sulfurreducens* pili. *Sci. Rep.* **6**, 23385 (2016).
25. Shipps, C. et al. Intrinsic electronic conductivity of individual atomically resolved amyloid crystals reveals micrometer-long hole hopping via tyrosines. *Proc. Natl Acad. Sci. USA* **118**, e2014139118 (2021).
26. Mehta, T., Childers, S. E., Glaven, R., Lovley, D. R. & Mester, T. A putative multicopper protein secreted by an atypical type II secretion system involved in the reduction of insoluble electron acceptors in *Geobacter sulfurreducens*. *Microbiology* **152**, 2257–2264 (2006).
27. Shi, L. et al. Direct involvement of type II secretion system in extracellular translocation of *Shewanella oneidensis* outer membrane cytochromes MtrC and OmcA. *J. Bacteriol.* **190**, 5512–5516 (2008).
28. Bouhenni, R. A. et al. The role of *Shewanella oneidensis* MR-1 outer surface structures in extracellular electron transfer. *Electroanalysis* **22**, 856–864 (2010).
29. Liu, X., Ye, Y., Xiao, K., Rensing, C. & Zhou, S. Molecular evidence for the adaptive evolution of *Geobacter sulfurreducens* to perform dissimilatory iron reduction in natural environments. *Mol. Microbiol.* **113**, 783–793 (2020).
30. Craig, L., Forest, K. T. & Maier, B. Type IV pili: dynamics, biophysics and functional consequences. *Nat. Rev. Microbiol.* **17**, 429–440 (2019).